



Year: 2020

Density, heterogeneity and deformability of red cells as markers of clinical severity in hereditary spherocytosis

Huisjes, Rick ; Makhro, Asya ; Llaudet-Planas, Esther ; Hertz, Laura ; Petkova-Kirova, Polina ; Verhagen, Liesbeth P ; Pignatelli, Silvia ; Rab, Minke A E ; Schiffelers, Raymond M ; Seiler, Elena ; van Solinge, Wouter W ; Vives Corrons, Joan-Luis ; Mañú-Pereira, Maria ; Kaestner, Lars ; Bogdanova, Anna ; van Wijk, Richard

Abstract: Hereditary spherocytosis originates from defective anchoring of the cytoskeletal network to the transmembrane protein complexes of the red blood cell. Red cells in hereditary spherocytosis are characterized by membrane instability, reduced deformability and a large heterogeneity in disease severity among patients. To unravel this variability in disease severity, we analyzed blood samples from 21 spherocytosis patients with defects in ankyrin, band 3, -spectrin and -spectrin using red cell indices, eosin-5-maleimide binding, microscopy and the osmotic fragility test, Percoll density gradients, vesiculation and ektacytometry to assess cell membrane stability, cellular density and deformability. Reticulocyte counts, CD71 abundance, band 4.1 a:b ratio, and HbA1c were used as markers of red blood cell turnover. We observed that patients with moderate/severe spherocytosis have short-living erythrocytes of low density and abnormally high intercellular heterogeneity. These cells show a prominent decrease in membrane stability and red cell deformability and, as a consequence, are quickly removed from the circulation by the spleen. In contrast, in mild spherocytosis less pronounced reduction in deformability results in prolonged red cell life-span and, hence, cells are subject to progressive loss of membrane. Red blood cells from patients with mild spherocytosis thus become denser before they are taken up by the spleen. Based on our findings, we conclude that red blood cell membrane loss, cellular heterogeneity and density are strong markers of clinical severity in spherocytosis.

DOI: <https://doi.org/10.3324/haematol.2018.188151>

Posted at the Zurich Open Repository and Archive, University of Zurich

ZORA URL: <https://doi.org/10.5167/uzh-175786>

Journal Article

Accepted Version

Originally published at:

Huisjes, Rick; Makhro, Asya; Llaudet-Planas, Esther; Hertz, Laura; Petkova-Kirova, Polina; Verhagen, Liesbeth P; Pignatelli, Silvia; Rab, Minke A E; Schiffelers, Raymond M; Seiler, Elena; van Solinge, Wouter W; Vives Corrons, Joan-Luis; Mañú-Pereira, Maria; Kaestner, Lars; Bogdanova, Anna; van Wijk, Richard (2020). Density, heterogeneity and deformability of red cells as markers of clinical severity in hereditary spherocytosis. *Haematologica*, 105(2):338-347.

DOI: <https://doi.org/10.3324/haematol.2018.188151>



Density, heterogeneity and deformability of red cells as markers of clinical severity in hereditary spherocytosis

by Rick Huisjes, Asya Makhro, Esther Llaudet-Planas, Laura Hertz, Polina Petkova-Kirova, Liesbeth P Verhagen, Silvia Pignatelli, Minke AE Rab, Raymond M Schiffelers, Elena Seiler, Wouter W van Solinge, Joan-LLuis Vives Corrons, Maria Mañú-Pereira, Lars Kaestner, Anna Bogdanova, and Richard van Wijk

Haematologica 2019 [Epub ahead of print]

Citation: Rick Huisjes, Asya Makhro, Esther Llaudet-Planas, Laura Hertz, Polina Petkova-Kirova, Liesbeth P Verhagen, Silvia Pignatelli, Minke AE Rab, Raymond M Schiffelers, Elena Seiler, Wouter W van Solinge, Joan-LLuis Vives Corrons, Maria Mañú-Pereira, Lars Kaestner, Anna Bogdanova, and Richard van Wijk. Density, heterogeneity and deformability of red cells as markers of clinical severity in hereditary spherocytosis.

Haematologica. 2019; 104:xxx

doi:10.3324/haematol.2018.188151

Publisher's Disclaimer.

E-publishing ahead of print is increasingly important for the rapid dissemination of science. Haematologica is, therefore, E-publishing PDF files of an early version of manuscripts that have completed a regular peer review and have been accepted for publication. E-publishing of this PDF file has been approved by the authors. After having E-published Ahead of Print, manuscripts will then undergo technical and English editing, typesetting, proof correction and be presented for the authors' final approval; the final version of the manuscript will then appear in print on a regular issue of the journal. All legal disclaimers that apply to the journal also pertain to this production process.

Density, heterogeneity and deformability of red cells as markers of clinical severity in hereditary spherocytosis

Authors: Rick Huisjes¹, Asya Makhro², Esther Llaudet-Planas³, Laura Hertz⁴, Polina Petkova-Kirova⁴, Liesbeth P Verhagen¹, Silvia Pignatelli¹, Minke AE Rab¹, Raymond M Schiffelers¹, Elena Seiler², Wouter W van Solinge¹, Joan-LLuis Vives Corrons³, Maria Mañú-Pereira³, Lars Kaestner^{4,5}, Anna Bogdanova², Richard van Wijk¹

Affiliations: ¹Department of Clinical Chemistry and Haematology, University Medical Center Utrecht, Utrecht University, Utrecht, The Netherlands. ²Red Blood Cell Research Group, Institute of Veterinary Physiology, Vetsuisse Faculty and the Zurich Center for Integrative Human Physiology (ZIHP), University of Zurich, Zurich, Switzerland. ³Red Blood Cell defects and Hematopoietic disorders unit, Josep Carreras Leukaemia Research Institute, Badalona, Barcelona, Spain. ⁴Theoretical Medicine and Biosciences, Medical Faculty, Saarland University, Homburg/Saar, Germany. ⁵Experimental Physics, Saarland University, Saarbruecken, Germany.

Corresponding author and author responsible for reprint requests: Dr. R. van Wijk, Department of Clinical Chemistry and Haematology, Laboratory for Red Blood Cell Research, University Medical Center Utrecht, Utrecht, The Netherlands. Telephone: +31887557769, fax: +31887555418, R.vanWijk@umcutrecht.nl

Source of support: The research leading to these results has received funding from the European Seventh Framework Program under grant agreement number 602121 (CoMMiTMenT) and from European Union's Horizon 2020 research and innovation programme under grant agreement No 675115 — RELEVANCE — H2020-MSCA-ITN-2015/H2020-MSCA-ITN-2015.

Disclosure and/or conflict of interest: Not applicable

Author contribution: RH, AM, EL, RS, WvS, JLVS, MM, LK, AB and RvW designed the research.

RH, AM, EL, LH, PK, LV, SP, MR and SE performed the research. RH, AM and EL analyzed the data.

RH, AM, LK, AB and and RvW wrote the paper.

Word count abstract: 224

Word count manuscript: 3010

Word count methods: 485

Running title: phenotypic markers for hereditary spherocytosis

Abstract (224)

Hereditary spherocytosis originates from defective anchoring of the cytoskeletal network to the transmembrane protein complexes of the red blood cell. Red cells in hereditary spherocytosis are characterized by membrane instability, reduced deformability and a large heterogeneity in disease severity among patients. To unravel this variability in disease severity, we analyzed blood samples from 21 spherocytosis patients with defects in ankyrin, band 3, α -spectrin and β -spectrin using red cell indices, eosin-5-maleimide binding, microscopy and the osmotic fragility test, Percoll density gradients, vesiculation and ektacytometry to assess cell membrane stability, cellular density and deformability. Reticulocyte counts, CD71 abundance, band 4.1 a:b ratio, and HbA1c were used as markers of red blood cell turnover. We observed that patients with moderate/severe spherocytosis have short-living erythrocytes of low density and abnormally high intercellular heterogeneity. These cells show a prominent decrease in membrane stability and red cell deformability and, as a consequence, are quickly removed from the circulation by the spleen. In contrast, in mild spherocytosis less pronounced reduction in deformability results in prolonged red cell life-span and, hence, cells are subject to progressive loss of membrane. Red blood cells from patients with mild spherocytosis thus become denser before they are taken up by the spleen. Based on our findings, we conclude that red blood cell membrane loss, cellular heterogeneity and density are strong markers of clinical severity in spherocytosis.

Abbreviations

CDPA = citrate phosphate dextrose adenine

EI_{\max} = maximal elongation index

EMA = eosin-5'-maleimide

MCHC = mean corpuscular hemoglobin concentration

MCV = mean corpuscular volume

MPA = mean projected area

MPA DW = mean projected area distribution width

OFT = osmotic fragility test

O_{\min} = hypotonic osmolarity where EI is minimal

O_{hyper} = hypertonic osmolarity at 50% of EI_{\max}

RBCs = red blood cell

RBCVs = red blood cell-derived vesicles

RDW = red blood cell distribution width

Introduction

Hereditary spherocytosis (HS) is the most common form of chronic hereditary hemolytic anemia in the Caucasian population, with an estimated prevalence of 1:2000 – 1:5000¹⁻³. HS usually originates from mutations in *ANK1* (ankyrin), *SLC4A1* (band 3), *SPTA1* (α -spectrin), *SPTB* (β -spectrin) or *EPB42* (protein 4.2)¹. Anemia in HS may require transfusion(s) and in severe cases splenectomy. A characteristic feature of HS is red blood cell (RBC) membrane instability, which leads to membrane loss and formation of dense cells with reduced RBC deformability⁴⁻⁶. Increased RBC density is an important feature of HS⁷ and is, for example, reflected by increased mean corpuscular hemoglobin concentrations (MCHC)^{8,9}.

HS is a very heterogeneous RBC disorder, resulting from a wide range of molecular defects and characterized by a high degree of heterogeneity in RBC properties and disease severity⁸⁻¹². In fact, even for HS patients with identical mutations, considerable differences in disease-severity are reported. It therefore seems reasonable to assume that the heterogeneity in disease severity is not only a reflection of particular genotype but is also impacted by other factors that control RBC properties.

Healthy RBCs become increasingly dense during their lifespan^{13,14}, but this process is accelerated in HS¹. Shedding of essentially hemoglobin-free vesicles results in an increase in MCHC and a corresponding increase in RBC density and intracellular viscosity^{13,15}. Electrogenic potassium leak also contributes to RBC dehydration in HS patients and is not compensated by Na⁺ accumulation^{16,17}. As a result, intracellular K⁺ concentration in RBCs of patients \approx 13 mmol/L lower than in cells of healthy subjects¹⁶, which results in net ion and water loss. Compensatory

activation of Na,K-ATPase in RBCs of patients was insufficient to prevent the loss of K^+ and dissipation of K^+/Na^+ gradients. Function of other electroneutral ion transporters (KCC, NKCC, Na/Li exchanger) in RBCs of HS patients was reported to be indistinguishable from that of cells of healthy controls^{16,18}.

In this study, we investigated a unique and genetically well-diagnosed group of HS patients on which we performed an in-depth analysis of RBC properties in HS, such as membrane instability, cellular density, cellular heterogeneity, vesiculation, turnover and lifespan. The obtained data were then correlated to clinical manifestations of HS, in both non-splenectomized and splenectomized patients, in order to identify markers of disease severity. Our results indicate that clinical severity in HS cannot be solely attributed to the protein harboring the mutation, but rather to the stability of the whole cytoskeletal network. RBC density, heterogeneity and deformability were identified as potential markers of severity. We found that the presence of dense RBCs is strongly associated with a milder HS manifestation. We hypothesize that unstable RBCs from clinically more severe patients are removed from the circulation before they acquire the features of senescence.

Methods

Subjects

Patients previously diagnosed with HS were enrolled in the CoMMiTMenT-study (<http://www.rare-anaemia.eu/>). This study was approved by the Medical Ethical Research Board of the University Medical Center Utrecht, the Netherlands, under reference code 15/426M and by the Ethical Committee of Clinical Investigations of Hospital Clinic, Spain, (IDIBAPS) under reference code 2013/8436.

Hemocytometry analysis

Hemocytometry parameters were analyzed on the Abbott Sapphire cell analyzer (Abbott Diagnostics Division, Santa Clara, CA, USA) and ADVIA 2120 (Hematology System, Siemens Healthcare Diagnostics, Forchheim, Germany)

Capillary-based measurements of MCV and MCHC

Triplicates of heparinized blood samples were filled in capillaries and centrifuged for 5 min at 12.000 rpm (Hematocrit 20, Hettich Zentrifugen). MCV was calculated using the formula; $MCV = \text{hematocrit} / [\text{RBC number}]$ and MCHC was calculated using the formula; $MCHC = [\text{Hemoglobin}] / \text{hematocrit}$.

Separation on the Percoll density gradient and determination of intracellular potassium levels

Intact blood samples were layered over a 90% isotonic Percoll solution containing plasma-like components as described elsewhere¹⁹. Briefly, Percoll density gradient and RBC separation were performed during the centrifugation at 50.000g for 15 min. (Sorvall RC 5C plus, rotor SM-24).

Intracellular potassium was measured using the Instrumentation Laboratory IL943 Flame Photometer according to Jokinen *et al.*²⁰

Osmotic gradient ektacytometry, osmotic fragility test (OFT) and EMA-binding

Osmotic gradient ektacytometry measurements of RBCs from healthy controls and HS patients were obtained using the Osmoscan module on the Lorrca MaxSis (Mechatronics, The Zwaag, The Netherlands) as previously described^{5,21}. The OFT was carried out as previously described by Parpart *et al.*²² and the eosin-5-maleimide (EMA) binding was determined according to previously published protocols^{12,23}.

RBC production, heterogeneity, vesiculation and turnover rate markers

RBCs were stained with anti-CD71 and isotype controls and were subsequently measured using a BD FACS Gallios²⁴. HbA1c measurements is an established tool to acquire information about RBC clearance and RBC age in hemolytic anemia-research^{15,25}. HbA1c levels were measured using the Menarini/ARKRAY HA-8180V. Band 4.1a:b ratio was detected in RBC membrane lysates after protein separation on the inverse SDS-PAGE gel (15-7.5%) and visualization of protein bands using Coomassie blue staining. Microscopic evaluation of RBC projected area and its heterogeneity was performed as described elsewhere^{26,27}. RBC vesicles were measured from CDPA plasma¹⁹ by staining them with mouse anti-human CD235a-APC and measure them using the Beckman Coulter CytoFLEX flow cytometer (S.Fig 1).

Statistical analysis and phenotype correlations

One-Way ANOVA with Post Hoc correction (Tukey) was used to compare sample means and Fisher's Exact Test was used to test whether clinical severity was proportionally distributed along the different genotypes. In non-splenectomized patients, clinical severity was assessed based on 1) hemoglobin and 2) reticulocytes levels which was previously defined by Bolton-Maggs *et al.*¹¹ (i.e. mild and moderate/severe). To prevent any confounders by splenectomized patients (designated as red dots), phenotype correlations were only carried out for unsplenectomized HS patients. Significant differences are depicted with horizontal bars, and significance levels are noted with * ($P \leq 0.05$), + ($P \leq 0.01$) or ‡ ($P \leq 0.001$).

Results

Baseline characteristics and red cell features of HS patients

Twenty-one patients with HS were included in this study and categorized according to clinical severity (Table 1)¹¹. HS was confirmed by targeted NGS of the seven genes most commonly mutated in HS (van Vuren *et al.*, in press). Splenectomy or a moderate/severe expression of disease was statistically overrepresented in patients with mutations in *ANK1* and *SPTB* ($P < 0.05$). Therefore, the phenotypic expression of HS due to *ANK1* and *SPTB* mutations appears to be more severe than HS due to *SLC4A1* and/or *SPTA1* defects. Decreased EMA staining, reflecting band 3 protein loss, was seen in all patients. Patients with *SPTA1* mutations tended to have higher EMA staining (Fig 1a), although the number of patients is too low to draw firm conclusions. The maximal deformability of RBCs, reflected by a decrease in EI_{max} as determined by the osmoscan, was decreased in all HS patients compared to healthy controls. This decrease was more pronounced in patients with *ANK1* and *SPTB* mutations compared to patients with mutations in *SPTA* or *SCL4A1* (Fig 1b). On the other hand, cells from patients with *SLC4A1* mutations tended to be more dehydrated as the O_{hyper} value was lower compared with both control blood samples and patients with *SPTA1* mutations (Fig 1c). The latter patients also showed the least pronounced loss of surface area-to-volume ratio, reflected by a normal O_{min} (Fig 1d) on the Osmoscan and normal results from the osmotic fragility test (50% lysis point) (Fig 1e). Membrane stability was compromised in all other HS patients.

As expected, RBC turnover was increased in all patients: reticulocyte counts were high (Table 1) and aging marker band 4.1a:b ratio was below that from healthy controls in all patients (Table 1).

The heterogeneity of the RBCs, reflected by the red blood cell distribution width (RDW), was increased compared to healthy controls (Fig 1f) as was the MCHC (Fig 1g). Intracellular K⁺ content was reduced in all patients but tended to be higher in HS patients with *SPTA1* mutations (Fig 1h).

An increase in heterogeneity in cell projected areas (MPA DW, Fig 2a) and a decrease in absolute mean values in projected area (MPA, Fig 2b) was seen in all HS patients compared to controls. Patients with *SLC4A1* and *SPTA1* mutations had cellular projected areas more similar to the healthy control group (Fig 2a,b). Patients with HS presented with higher heterogeneity in cell density compared with healthy subjects, showing more sub-fractions of M fraction and a broader distribution width of the M fraction (Fig 2c-e). These changes were more pronounced in patients with mutations in *ANK1* and *SPTA1*. Furthermore, the M fraction of patients with *SLC4A1* mutations was lower than the cells of healthy controls, compared to the other HS patients (Fig 2f, S.Fig 2).

In summary, specific changes were observed in parameters associated with membrane stability, stiffness and deformability, as well as RBC heterogeneity of RBCs in our cohort of HS patients.

RBC markers of severity of HS

As described in Table 1, severity of HS in non-splenectomized patients was determined based on the decrease in hemoglobin levels and increase in reticulocyte counts¹¹. In our patients Hb levels positively correlated with MCHC levels (Fig 3a). An inverse correlation was observed between Hb and RDW (Fig 3b), and Hb and reticulocyte counts (Fig 3c). Furthermore, an inverse correlation

was observed between Hb and parameters defining RBC hydration status such as intracellular K^+ or O_{hyper} (Fig d, e).

Decreases in RBC life-span was assessed by a reduction in changes in HbA1c in severe nonsplenectomized HS patients, whereas in patients with mild disease manifestation or in splenectomized patients HbA1c levels were within the normal range (Fig 4a).

Patients with moderate/severe HS had less deformable RBCs reflected by lower El_{max} values than patients with mild HS or splenectomized patients (Fig 4b). Red blood cells of mild HS patients also tended to be more dehydrated based on the O_{hyper} measurements (Fig 4c). In line with this, patients with mild HS showed higher MCHC values than moderate/severely affected patients (Fig 4d) and had higher density of M fraction based on its position within the Percoll gradient (Fig 4e, S.Fig 2).

Membrane loss was more pronounced in patients with moderate/severe HS based on reduced MPA (Fig 4f). In line with this, the number of RBCVs detected in plasma of moderate-severe HS patients was higher than in patients with mild HS (Fig 4g). No difference in EMA staining was however observed between mild and moderate/severe HS (Fig 4c). Inter-cellular heterogeneity (RDW and MPA DW) was increased in moderate-severe HS patients compared with mild HS patients and healthy controls (Fig 4i, j).

In summary, patients with more severe expression of the disease had red cells with reduced life span and less stable membrane. Cells were smaller and more heterogeneous in size and density. Strikingly, patients with mild HS had red blood cells that were more dense and had higher MCHC values (Fig 4d, e).

Effect of splenectomy on RBC markers of severity

Splenectomy performed in moderate-severe HS patients results in an increase in Hb levels and erythrocyte counts (data not shown). In our cohort it also is associated with a decrease in RDW (Fig 5a, and normalization of RBC morphology (S.Fig 3, S.Fig 4)). Survival of RBCs from splenectomized HS patients, as assessed by HbA1c content or band 4.1a:b ratio, was found to be increased (Fig 5b, 5c).

Several parameters remained unaffected by splenectomy. Splenectomy did not alter MCHC (Fig d) or intracellular K^+ levels (Fig 5e) and did not correct band 3 loss (Fig 5f). It also did not affect deformability (no effect on El_{max} and O_{hyper}) (Fig 5g,h). However, the cells did survive for longer time in the circulation despite an increase in osmotic fragility (Fig 5i).

Discussion

This comprehensive study on a well-characterized cohort of patients offers insight into the variable phenotypic manifestations of HS, possible causes of clinical heterogeneity, and severity or the impact of splenectomy. We show here that strong markers of moderate/severe expression of HS are (1) lower RBC density, reflected by differences in MCHC and fractionation of RBCs on the Percoll density gradient, (2) reduced RBC deformability and increased membrane loss as determined by RBC vesicle numbers and a decrease in MPA, and (3) heterogeneity in RBC population reflected by differences in RDW and fractionation of RBCs using a Percoll gradient.

We conclude that patients with moderate/severe HS have short-lived RBCs of lower density and abnormally high intercellular heterogeneity, whereas in mild HS less pronounced reduction in deformability results in prolonged RBC life-span and, hence, cells are exposed to progressive loss of membrane. RBCs from patients with mild HS thus become more dense before they are taken up by the spleen.

Genotype to phenotype correlations in HS

While previous studies were limited to protein analysis by SDS-page¹², we used Next-Generation Sequencing to establish the cause of HS. This enabled us to clearly establish the primary genetic defect, in contrast to other conventional techniques like SDS-page which may lead to confounding results as it may be influenced by secondary protein defects in HS. Regardless of the underlying mutation all patients shared common features like increases in reticulocyte counts and MCHC, dehydration and an increase in RBC density, increased heterogeneity and overall reduction in deformability due to the destabilisation of cytoskeletal structure^{1,28}. We also

observed that red cell size, intracellular K⁺ content and reticulocyte counts did not differ between patients with *SLC4A1*, *ANK1*, *SPTB* and *SPTA1* mutations (Fig 1h, Fig 2b, Table 1). Within one group of patients with the same protein mutated we noted marked differences in severity and clinical manifestation of the disease, the *ANK1* group being the most diverse of all. We also noted that patients with *SPTA1* mutations had a less severe phenotype (i.e. based on Hb levels, reticulocyte count, RDW, intracellular K⁺, and EMA staining) compared to the other patients. This is in contrast with the more severe disease phenotype of *SPTA1* mutations reported in other studies²⁹. Similarly, our patients with *SPTB* mutations presented with normal MCHC values, whereas in other studies MCHC was shown to be elevated in patients carrying *SPTB* mutations³⁰. Due to the relatively small numbers of patients within each group we can not draw firm conclusions on the link between genotype and phenotypic expression.

RBC density as a marker of clinical severity

Decreased Hb, Hct and RBC counts associated with increased markers of hemolysis and erythropoietic activity were previously reported as markers for HS severity⁹. Among the molecular mechanisms defining HS severity a major role was assigned to RBC membrane instability and loss of membrane proteins²⁸ (MCHC, EMA test, SDS-PAGE), along with decreased deformability as measured by osmotic gradient ektacytometry⁵. In our cohort, increased severity was associated with membrane instability and extensive membrane and band 3 protein loss over a shorter time (Fig 4b,g-i). RBC turnover in severe HS patients was reflected by a decrease in HbA1c levels exceeding those in patients with mild HS (Fig 4a). The RBCs in patients with

moderate/severe HS had lower MCHC than those of mild HS patients (Fig 3a, 4d). The average M fraction density for moderate/severe HS patients RBCs did not differ from cells of healthy controls, whereas cells of mild HS patients showed an increase in density (Fig 4e) and lower deformability as they “aged”, spending more time in the circulation getting more “senescent” than highly unstable cells of severe HS patients. Thus, life span and decrease in El_{max} appeared to be a reliable marker of disease severity (Fig 4b), regardless of the genotype.

Delayed clearance of RBCs in patients with mild HS allowed them to lose membrane more gradually (Fig 4g, S.Fig 3), which results in a better conservation of RBC deformability (Fig 4b) and the ability form dense cells (Fig 4c-e, S.Fig 2). Direct measurements of membrane shedding by monitoring the plasma-borne vesicles is challenging due to their fast sequestration and clearance^{31–33}. However, higher levels of circulating RBCVs were detected in plasma from moderate/severe HS patients(Fig 4g). These findings are in line with an increase in other markers of membrane loss, such as changes in gross morphology toward spherocytic (S.Fig 3), as well as higher number of microcytes as detected by quantitative digital microscopy (S.Fig 4).

RBC heterogeneity and deformability as a marker of clinical severity

One more parameter we found to reflect disease severity in HS is RBC heterogeneity. Increases in RDW, RDW/Hb and MCHC/RDW ratio were suggested as HS markers for clinical severity⁹. In our study RDW correlated with HS severity as well (Fig 3b). Absolute RDW values are known to vary between labs and depend on the age and physical activity of the subjects³⁴. We therefore used microscopy and indeed patients with severe HS had a broader range of RBC

shapes and MPA DW (Fig 4 j, S.Fig 3).

Word of caution for automatic detection of hematocrit and MCHC in HS patients

MCHC was previously suggested to be prognostic for the severity of HS in non-splenectomized patients^{9,11}. For the measurements of MCHC, we used a capillary-based method for hematocrit detection. In line with previous observations³⁵⁻³⁷ we found that automated measurements of MCHC of pathological RBCs are imprecise for HS patients (see S.Fig 5). Inaccuracy of automated MCHC detection of dehydrated RBC has been discussed for over 30 years³⁵. It results from a substantial overestimation of MCV, both values being based on hematocrit detection or calculations methods^{38,39}. As mentioned previously, others have shown that increased hemoglobin concentrations are equivalent to milder disease severity scores in HS^{9,11}. We show that MCHC values calculated based on the capillary hematocrit correlated with blood hemoglobin content (Figs 1g, 3a, 4d).

Conclusions

This study reveals the factors defining RBC longevity and erythropoietic activity in patients with HS. These are membrane stability, which in turn depends on the localization of mutations impacting vertical or horizontal interactions within the membrane cytoskeleton and on the presence of splenic filtering capacity. Mild HS is associated with prolonged survival of RBCs in the circulation and allows to RBCs in mild HS to lose more membrane, which results in smaller and denser RBCs. Shorter-lived unstable RBCs of patients with severe HS phenotype are more heterogeneous and less dense, as reflected by lower MCHC.

Parameters that specifically mark clinical severity in HS are summarized in Table 2 and consist of RBC density (MCHC, Percoll, O_{hyper}), RBC deformability (EI_{max}), and RBC heterogeneity (RDW). They may be used to monitor the success of supportive therapy and assist in the development of new personalized treatment regimens.

Acknowledgments

The research leading to these results has received funding from the European Seventh Framework Program under grant agreement number 602121 (CoMMiTMeNT) and from the European Union's Horizon 2020 research and innovation programme under grant agreement No 675115 — RELEVANCE — H2020-MSCA-ITN-2015/H2020-MSCA-ITN-2015.

References

1. Perrotta S, Gallagher PG, Mohandas N. Hereditary spherocytosis. *Lancet*. 2008;372(9647):1411–1426.
2. Morton NE, Mackinnon A, Kosower N, Schilling RF, Gray MP. Genetics of spherocytosis. *Am J Hum Genet*. 1962;170–184.
3. Gallagher PG. Hereditary Elliptocytosis: Spectrin and Protein 4.1R. *Semin Hematol*. 2004;41(2):142–164.
4. Da Costa L, Mohandas N, Sorette M, Grange MJ, Tchernia G, Cynober T. Temporal differences in membrane loss lead to distinct reticulocyte features in hereditary spherocytosis and in immune hemolytic anemia. *Blood*. 2001;98(10):2894–2899.
5. Lazarova E, Gulbis B, Oirschot B van, van Wijk R. Next-generation osmotic gradient ektacytometry for the diagnosis of hereditary spherocytosis: interlaboratory method validation and experience. *Clin Chem Lab Med*. 2017;55(3):394–402.
6. Huisjes R, Bogdanova A, van Solinge WW, Schiffelers RM, Kaestner L, van Wijk R. Squeezing for Life – Properties of Red Blood Cell Deformability. *Front Physiol*. 2018;9:656.
7. Michaels LA, Cohen AR, Zhao H, Raphael RI, Manno CS. Screening for hereditary spherocytosis by use of automated erythrocyte indexes. *J Pediatr*. 1997;130(6):957–960.
8. Cynober T, Mohandas N, Tchernia G. Red cell abnormalities in hereditary spherocytosis: Relevance to diagnosis and understanding of the variable expression of clinical severity. *J Lab Clin Med*. 1996;128(3):259–269.
9. Rocha S, Costa E, Rocha-Pereira P, et al. Complementary markers for the clinical severity classification of hereditary spherocytosis in unsplenectomized patients. *Blood Cells Mol Dis*. 2011;46(2):166–170.
10. Eber SW, Armbrust R, Schröter W. Variable clinical severity of hereditary spherocytosis: Relation to erythrocytic spectrin concentration, osmotic fragility, and autohemolysis. *J Pediatr*. 1990;117(3):409–416.
11. Bolton-Maggs PHB, Langer JC, Iolascon A, Tittensor P, King M-J, General Haematology Task Force of the British Committee for Standards in Haematology. Guidelines for the diagnosis and management of hereditary spherocytosis - 2011 update. *Br J Haematol*. 2012;156(1):37–49.
12. King MJ, Behrens J, Rogers C, Flynn C, Greenwood D, Chambers K. Rapid flow cytometric test for the diagnosis of membrane cytoskeleton-associated haemolytic anaemia. *Br J Haematol*. 2000;111(3):924–933.
13. Bosch FH, Werre JM, Schipper L, et al. Determinants of red blood cell deformability in relation to cell age. *Eur J Haematol*. 1994;52(1):35–41.

14. Waugh RE, Narla M, Jackson CW, Mueller TJ, Suzuki T, Dale GL. Rheologic properties of senescent erythrocytes: loss of surface area and volume with red blood cell age. *Blood*. 1992;79(5):1351–1358.
15. Bosman GJCGM. Survival of red blood cells after transfusion: processes and consequences. *Front Physiol*. 2013;4:376.
16. Vives Corrons JL, Besson I. Red cell membrane Na⁺ transport systems in hereditary spherocytosis: relevance to understanding the increased Na⁺ permeability. *Ann Hematol*. 2001;80(9):535–539.
17. Gallagher PG. Disorders of erythrocyte hydration. *Blood*. 2017;130(25):2699–2708.
18. De Franceschi L, Olivieri O, Miraglia del Giudice E, et al. Membrane cation and anion transport activities in erythrocytes of hereditary spherocytosis: effects of different membrane protein defects. *Am J Hematol*. 1997;55(3):121–128.
19. Makhro A, Huisjes R, Verhagen LP, et al. Red Cell Properties after Different Modes of Blood Transportation. *Front Physiol*. 2016;7:288.
20. Jokinen CH, Swaim WR, Nuttall FQ. A case of hereditary xerocytosis diagnosed as a result of suspected hypoglycemia and observed low glycohemoglobin. *J Lab Clin Med*. 2004;144(1):27–30.
21. Da Costa L, Suner L, Galimand J, et al. Diagnostic tool for red blood cell membrane disorders: Assessment of a new generation ektacytometer. *Blood Cells Mol Dis*. 2016;56(1):9–22.
22. Parpart AK, Lorenz PB, Parpart ER, Gregg JR, Chase AM. The osmotic resistance (fragility) of human red cells. *J Clin Invest*. 1947;26(4):636–640.
23. King M-J, Telfer P, MacKinnon H, et al. Using the eosin-5-maleimide binding test in the differential diagnosis of hereditary spherocytosis and hereditary pyropoikilocytosis. *Cytometry B Clin Cytom*. 2008;74(4):244–250.
24. Ghosh S, Chakraborty I, Chakraborty M, Mukhopadhyay A, Mishra R, Sarkar D. Evaluating the morphology of erythrocyte population: An approach based on atomic force microscopy and flow cytometry. *Biochim Biophys Acta*. 2016;1858(4):671–681.
25. Lutz HU, Bogdanova A. Mechanisms tagging senescent red blood cells for clearance in healthy humans. *Front Physiol*. 2013;4:387.
26. Makhro A, Kaestner L, Bogdanova A. NMDA Receptor Activity in Circulating Red Blood Cells: Methods of Detection. *Methods Mol Biol*. 2017;1677:265–282.
27. Huisjes R, van Solinge WW, Levin MD, van Wijk R, Riedl JA. Digital microscopy as a screening tool for the diagnosis of hereditary hemolytic anemia. *Int J Lab Hematol*. 2018;40(2):159–168.

28. Narla J, Mohandas N. Red cell membrane disorders. *Int J Lab Hematol*. 2017;39 Suppl 1:47–52.
29. Chonat S, Risinger M, Dagaonkar N, et al. The Spectrum of Alpha-Spectrin Associated Hereditary Spherocytosis. *Blood*. 2015;126(23):941.
30. Maciag M, Płochocka D, Adamowicz-Salach A, Burzyńska B. Novel beta-spectrin mutations in hereditary spherocytosis associated with decreased levels of mRNA. *Br J Haematol*. 2009;146(3):326–332.
31. Willekens FLA, Werre JM, Groenen-Döpp YAM, Roerdinkholder-Stoelwinder B, de Pauw B, Bosman GJCGM. Erythrocyte vesiculation: a self-protective mechanism? *Br J Haematol*. 2008;141(4):549–556.
32. Ciana A, Achilli C, Gaur A, Minetti G. Membrane Remodelling and Vesicle Formation During Ageing of Human Red Blood Cells. *Cell Physiol Biochem*. 2017;42(3):1127–1138.
33. Willekens FLA, Werre JM, Kruijt JK, et al. Liver Kupffer cells rapidly remove red blood cell-derived vesicles from the circulation by scavenger receptors. *Blood*. 2005;105(5):2141–2145.
34. Salvagno GL, Sanchis-Gomar F, Picanza A, Lippi G. Red blood cell distribution width: A simple parameter with multiple clinical applications. *Crit Rev Clin Lab Sci*. 2015;52(2):86–105.
35. Mohandas N, Clark MR, Kissinger S, Bayer C, Shohet SB. Inaccuracies associated with the automated measurement of mean cell hemoglobin concentration in dehydrated cells. *Blood*. 1980;56(1):125–128.
36. Berda-Haddad Y, Faure C, Boubaya M, et al. Increased mean corpuscular haemoglobin concentration: artefact or pathological condition? *Int J Lab Hematol*. 2017;39(1):32–41.
37. Zandecki M, Genevieve F, Gerard J, Godon A. Spurious counts and spurious results on haematology analysers: a review. Part II: white blood cells, red blood cells, haemoglobin, red cell indices and reticulocytes. *Clin Lab Haematol*. 2007;29(1):21–41.
38. Kokholm G. Simultaneous measurements of blood pH, $p\text{CO}_2$, $p\text{O}_2$ and concentrations of hemoglobin and its derivatives-A multicenter study. *Scand J Clin Lab Invest*. 1990;50(sup203):75–86.
39. O'Connor G, Molloy AM, Daly L, Scott JM. Deriving a useful packed cell volume estimate from haemoglobin analysis. *J Clin Pathol*. 1994;47(1):78–79.

Table legends

Table 1: hemocytometry, chemistry parameters, cell-age markers and genotypes of mild, moderate/severe and splenectomized HS patients included in this study. Clinical severity in non-splenectomized HS patients was assigned according to Bolton-Maggs *et al.*¹¹ on basis of 1) hemoglobin and 2) reticulocytes levels. Mild HS was defined as hemoglobin levels between 110–150 g/L, moderate HS as hemoglobin levels between 80–120 g/L and severe HS as hemoglobin levels lower than 80 g/L. HS patients with hemoglobin levels between 110 and 120 were categorized as mild or moderate on basis of their reticulocytes levels (i.e. lower or higher than 6% reticulocytes). Novel mutations are displayed in bold face and the pathogenicity of novel missense variants predicted with SIFT, PolyPhen-2, and MutationTaster (results not shown). Notation of α^{LELY} represents *SPTA1* c.[5572C>G; 6531-12C>T] p.[(Leu1858Val);(?)].

Table 2: summary of parameters that characterize disease severity in HS. Symbol (↑) indicates increased compared to healthy controls, (↓) indicates decreased compared to healthy controls and (=) indicates equal to healthy controls.

Tables

N	Sex	Age	Genotype	Hb (g/dL)	RBC (10 ¹² /L)	Hct (%)	MCV (fL)	Ret (%)	MCHC (g/L)	RDW (%CV)	EMA (%)	O _{min} (mOsmol/L)	EI _{max} (A.U.)	O _{hyper} (mOsmol/L)	OFT (g/L NaCl)	Band 4.1/4.2 ratio (A.U)	CD71 (%)
Mild HS ¹¹																	
1	♂	75	ANK1 c.344T>C p.Leu115Pro	136	4,1	n.a	n.a	7,2	n.a	16,2	85	162	0,555	457	7,0	0,70	0,8
2	♂	46	SLC4A1 c.1030C>T p.Arg344*	153	4,7	n.a	n.a	3,2	n.a	15,2	71	163	0,563	417	6,6	0,87	1,4
3	♂	40	SLC4A1 c.1421C>A p.Ala474Asp	140	4,9	n.a	n.a	4,0	n.a	12,3	93	162	0,557	427	5,7	0,99	1,2
4	♀	55	SLC4A1 c.2057+1G>A (splicing)	136	4,0	36,5	91,1	7,8	372	14,0	73	158	0,554	405	6,4	0,82	2,7
5	♀	18	SLC4A1 c.2057+1G>A (splicing)	131	3,7	35,7	96,9	9,4	367	13,1	77	166	0,569	410	6,1	0,84	1,4
6	♂	58	SLC4A1 c.2348T>A p.Ile783Asn	132	4,1	36,5	88,4	8,9	363	15,7	68	169	0,548	429	6,8	n.a	3,5
7	♂	40	SPTA1 c.678G>A p.Glu227fs + α ^{LELY}	127	4,1	35,9	87,8	5,8	355	15,0	94	175	0,600	453	5,6	0,84	0,9
8	♂	54	SPTA1 c.[4339-99C>T; c.4347G>T] p.[(?; Lys1449Asn)]; c.4339-99C>T p.(?)	121	3,5	34,7	98,3	3,9	348	15,3	94	160	0,566	458	5,7	n.a	0,9
Moderate/severe HS ¹¹																	
9	♂	4	ANK 1 c.341C>T p.Pro114Leu	116	3,8	30,0	80,1	9,1	386	14,5	72	162	0,509	398	6,6	0,72	2,2
10	♀	3	ANK1 c.1943delC p.Ala648fs	117	4,02	36,3	90,4	11,9	321	21,1	59	164	0,503	424	6,6	n.a	0,2
11	♂	5	ANK1 c.2394_2397delCAGT p.Ser799fs	120	4,1	32,2	78,6	18,4	372	25,4	67	185	0,472	462	7,8	n.a	7,3
12	♀	26	ANK1 c.2559-2A>G (splicing)	102	3,3	29,4	89,5	18,3	346	24,1	84	170	0,537	446	6,4	0,60	5,3
13	♂	1	SPTB c.154delC p.Arg52fs	86	3,38	30,2	89,5	11,9	284	24,7	66	168	0,532	456	5,7	n.a	4,8
14	♂	3	SPTB c.2470C>T p.Gln824*	78	2,9	23,7	81,9	10,6	328	23,8	71	180	0,534	475	6,7	n.a	2,9
15	♂	4	SPTB c.5937+1G>A p.(?)	84	3,09	27,7	89,7	16,7	303	23,4	74	173	0,541	459	7,0	n.a	5,5
16	♀	42	SPTA1 c.2755G>T p.Glu919* + α ^{LELY}	113	3,5	31,7	91,8	8,2	355	16,0	89	178	0,567	471	5,9	n.a	2,1
Splenectomized HS ¹¹																	
17	♀	31	ANK1 c.341C>T p.Pro114Leu	152	4,9	84,7	41,9	8,4	362	11,8	76	179	0,533	437	7,4	1,08	0,1
18	♀	46	ANK1 c.344T>C p.Leu115Pro	143	4,6	n.a.	n.a.	2,8	n.a.	12,4	74	158	0,590	423	7,4	1,18	0,2
19	♀	84	SLC4A1 c.2057+1G>A (splicing)	160	4,8	121,8	45,1	12,6	354	11,0	67	164	0,565	417	7,1	1,07	0,2
20	♀	71	SPTB c.2136_2137delinsTT	164	4,84	100,9	48,8	2,2	337	13,2	77	173	0,509	445	7,3	0,99	0,3
21	♀	40	SPTB c.3449G>A p.Trp1150*	163	4,94	92,0	45,5	12,2	359	11,9	73	183	0,512	440	7,8	1,22	0,3

Table 1

Disease Severity	MCHC	Density (Percoll, O_{hyper})	RDW	Reticulocytes	Deformability (El_{max})	Membrane loss (vesiculation)
Mild	↑↑	↑↑	=	↑	↓	↑
Moderate/severe	↑	↑	↑↑	↑↑	↓↓	↑↑
Splenectomised	↑↑	=	=	↑	=	=

Table 2

Figure legends

Fig 1: basic characteristics (median \pm range) of healthy controls and HS patients. HS patients were grouped as one group and according to their affected genes (*ANK1* (ankyrin), *SLC4A1* (band 3), *SPTB* (β -spectrin) and *SPTA1* (α -spectrin)). Blue circles represent healthy controls, black circles represent (unsplenectomized) HS patients and red circles represent splenectomized HS patients. The gray range indicates the reference range for healthy controls. Panel a) EMA-binding (%), b) maximum deformability (EI_{max}), c) hydration state of the RBC reflected by O_{hyper} , d) osmotic fragility measured by osmotic gradient ektacytometry and reflected in the O_{min} , e) 50% lysis point in the osmotic fragility test, f) red blood cell distribution width (RDW) (%CV), g) MCHC by capillary measurements (g/L) (%CV), h) intracellular potassium (mmol/L). Significant differences are depicted with horizontal bars, and significance levels are noted with * ($P \leq 0.05$), + ($P \leq 0.01$) or ‡ ($P \leq 0.001$).

Fig 2: RBC heterogeneity in HS. RBC heterogeneity was measured in healthy controls and HS with microscopy (4a, 4b) and Percoll density gradients (4c-4f). HS patients were grouped according to their affected genes (*ANK1* (ankyrin), *SLC4A1* (band 3), *SPTB* (β -spectrin) and *SPTA1* (α -spectrin)). a) Mean Projected Area Distribution Width (MPA DW), b) Mean Projected Area (MPA), c) An example a blood sample from a patient with HS and a healthy control. On the samples the young RBC fraction, the main RBC fraction (fraction M) and dense RBC fractions are designated with green, blue and red lines. The M-fraction is subdivided in subfractions (M1, M2 etc). The position of the M fraction is calculated from the position of the most intense (a.u.) subfraction relative to the total length of Percoll column. The HS patient has 7 RBC subfractions, and the position of the

most intense subfraction (i.e. subfraction M3) is lower than in control (i.e. subfraction M1), d) The number of subfractions in the RBC density gradient, e) Fractions distribution width (%), f) Position of M fraction (%). Significant differences are noted by * ($P \leq 0.05$), † ($P \leq 0.01$) or ‡ ($P \leq 0.001$).

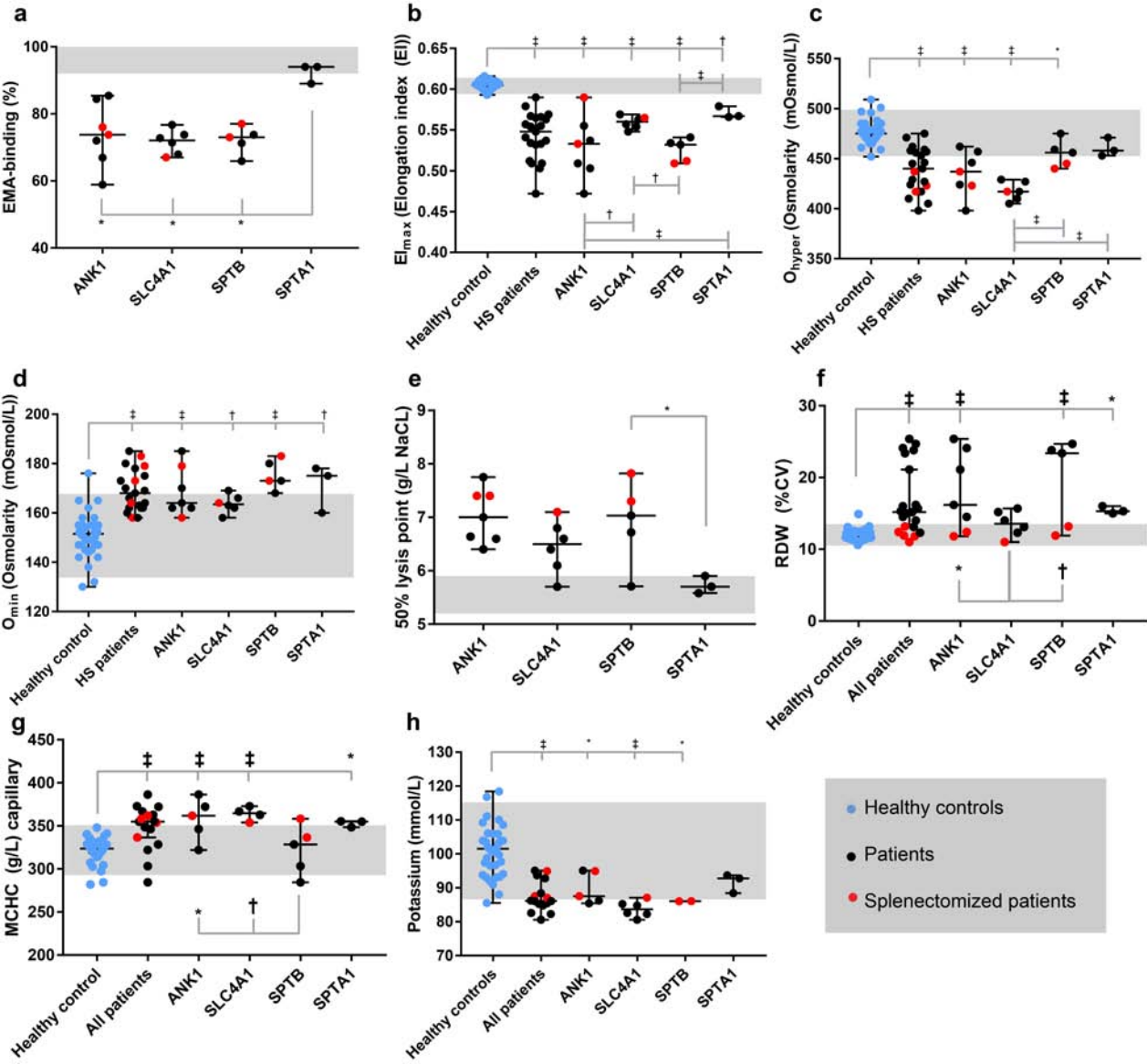
Fig 3: RBC parameters and their relationship to clinical severity in unsplenectomized HS patients.

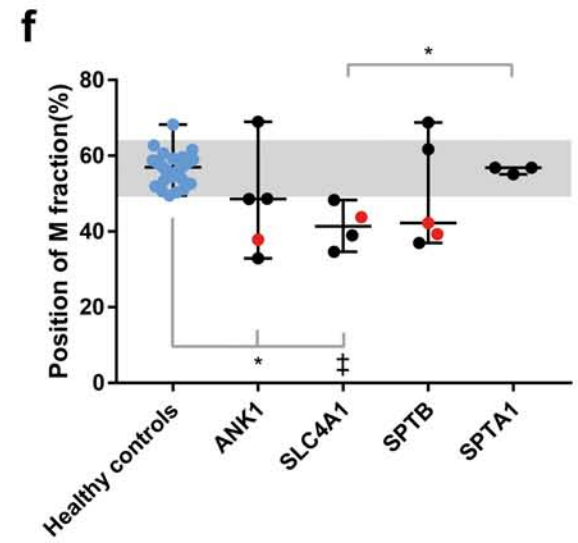
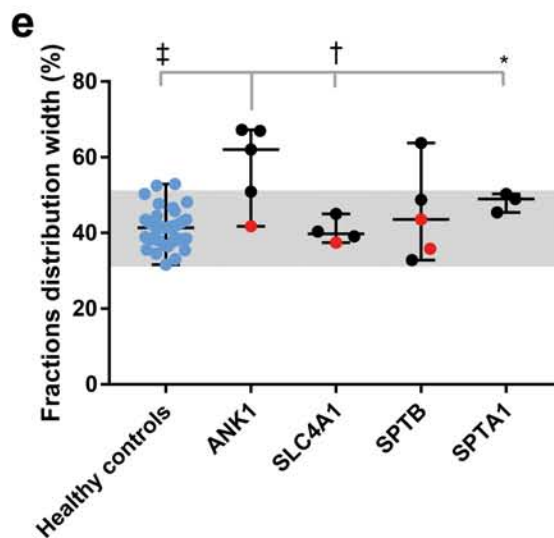
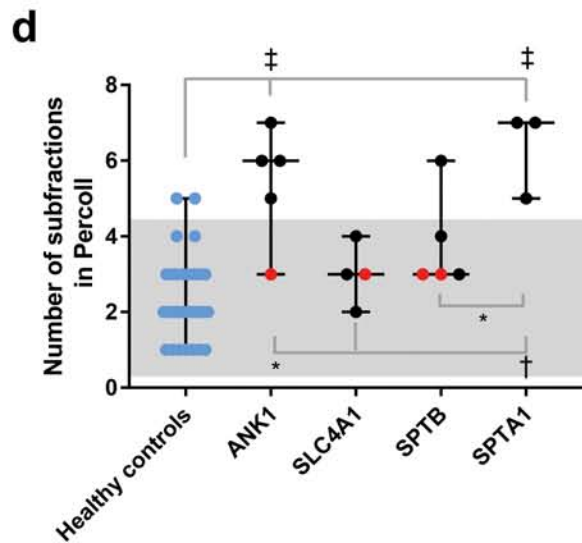
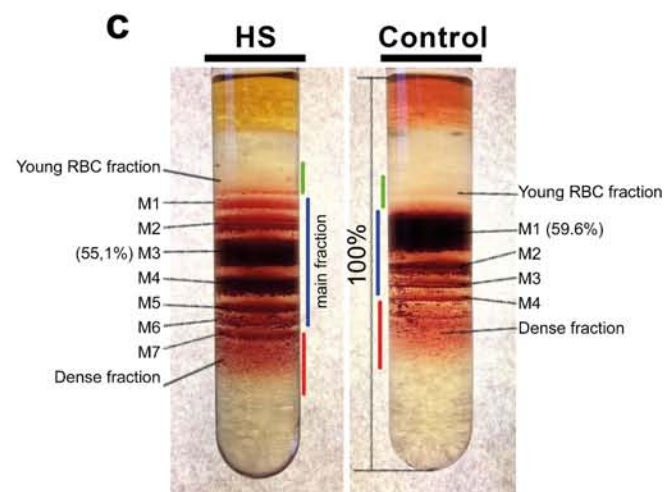
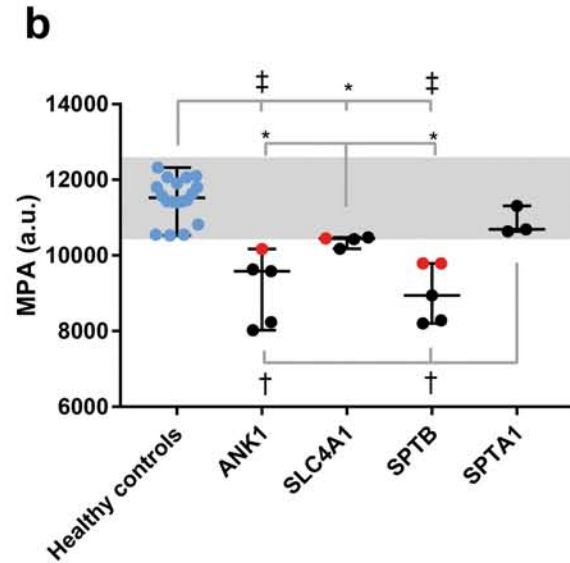
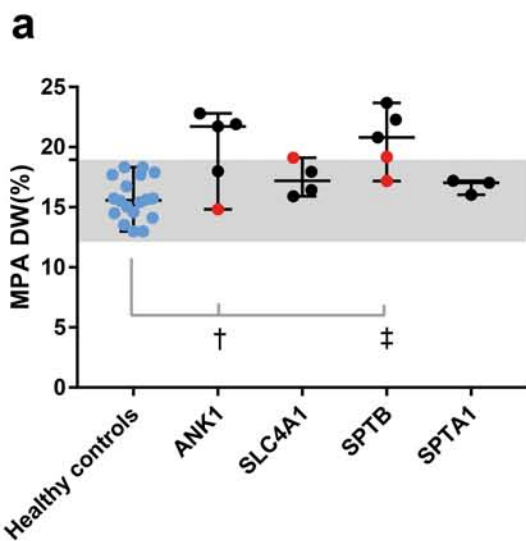
a) MCHC (g/L), b) RDW (%CV), c) Reticulocytes (%), d) intracellular potassium (mmol/L), e) O_{hyper} (mOsmol/L).

Fig 4: RBC density and stability as markers of severity in HS. HS patients are grouped on clinical severity (i.e. mild, moderate/severe and splenectomized) (reference range in gray area). a) HbA1c (mmol/mol), b) maximum deformability (EI_{max}), c) O_{hyper} (mOsmol/L), d) MCHC (g/L), e) Position of M fraction(%), f) Mean cell projected area (a.u.), g) RBC-vesicles (particles/ 10^{12} RBCs/L plasma), h) EMA-binding (%), i) RDW (%CV), j) Mean cell projected area distribution width (MPA DW). Significant differences are represented by horizontal bars, and significance levels are noted by * ($P \leq 0.05$), † ($P \leq 0.01$) or ‡ ($P \leq 0.001$).

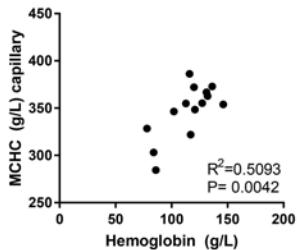
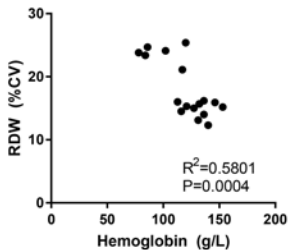
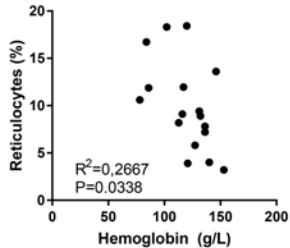
Fig 5: Role of splenectomy on RBC parameters in HS. Blue circles represent healthy controls, black circles represents (unsplenectomized) HS patients and red circles represent splenectomized HS patients. HS patients are grouped on clinical severity (i.e. mild, moderate/severe and splenectomized). a) RDW (%CV), b) HbA1c (mmol/mol), c) 4.1a/4.1b ratio, d) MCHC (g/L), e) intracellular potassium (mmol/L), f) EMA-binding hemoglobin (%), g) maximum deformability

($E_{I_{max}}$), h) hydration state of the RBC reflected by O_{hyper} (mOsmol/L), i) 50% lysis point in the OFT (g/L NaCl). Significant differences are noted by * ($P \leq 0.05$), + ($P \leq 0.01$) or ‡ ($P \leq 0.001$).

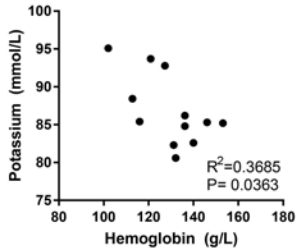
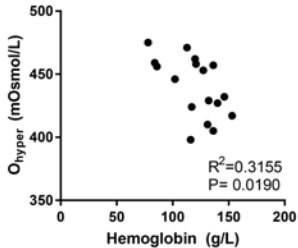


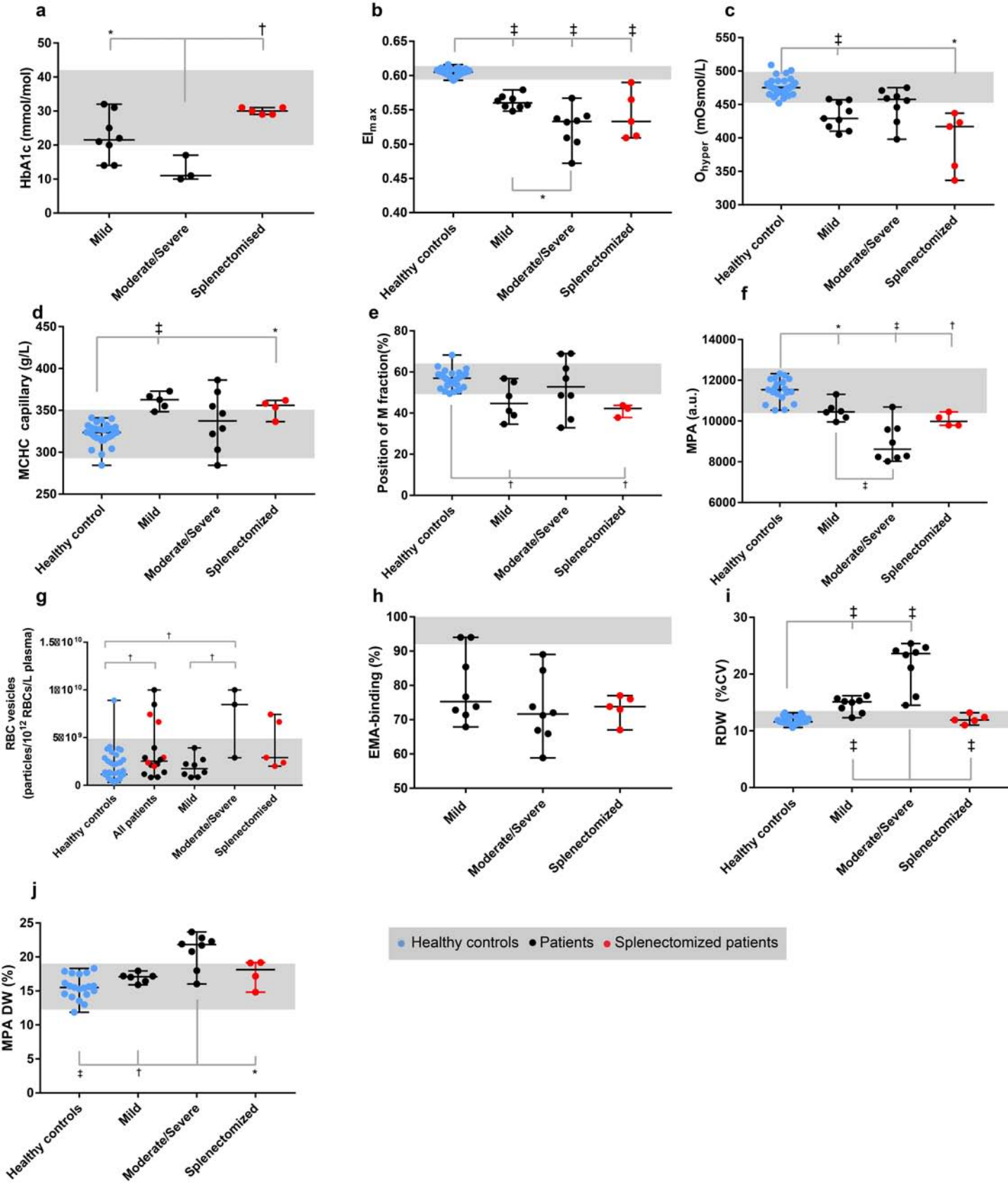


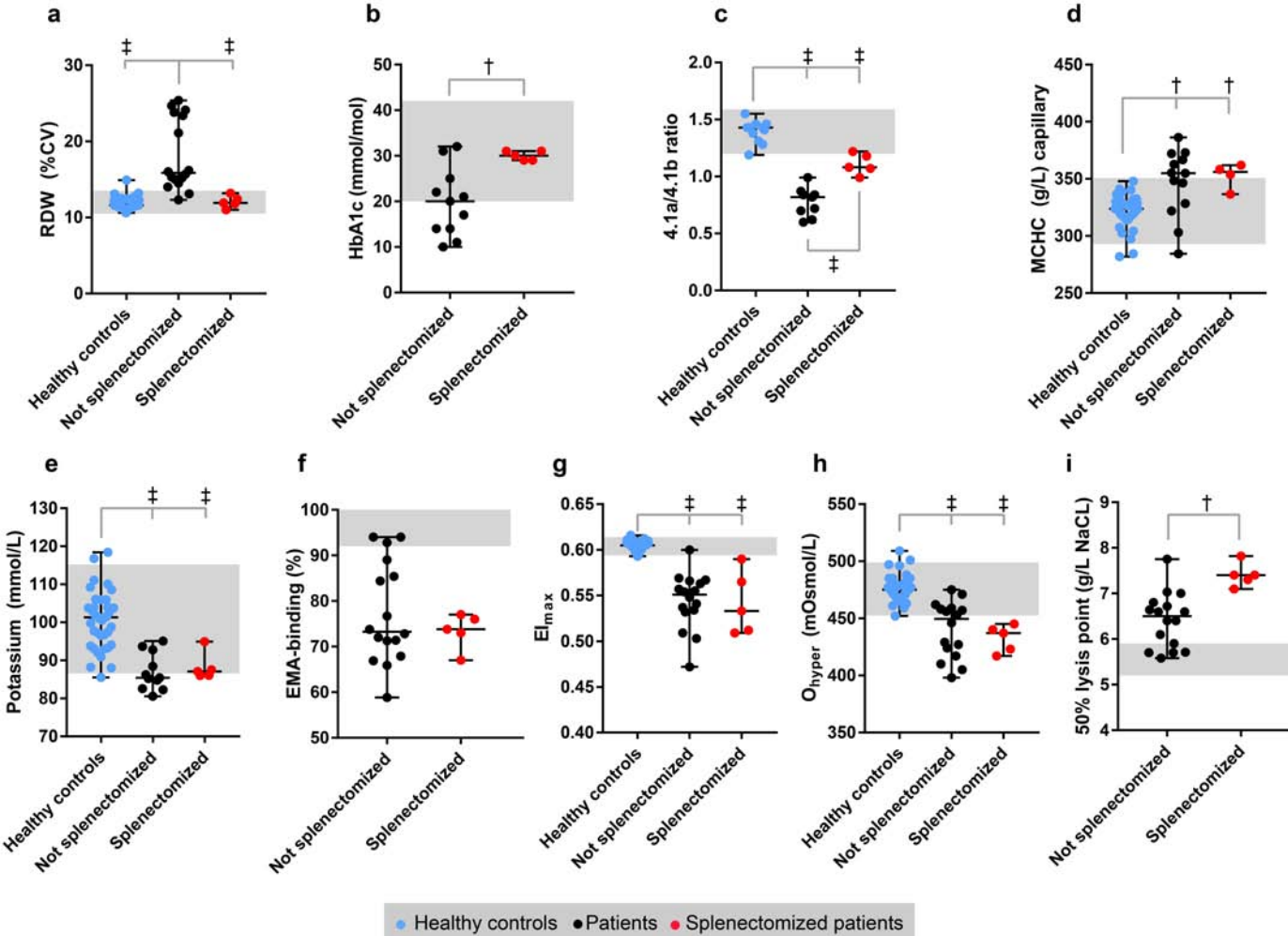
● Healthy controls ● Patients ● Splenectomized patients

a**b****c**

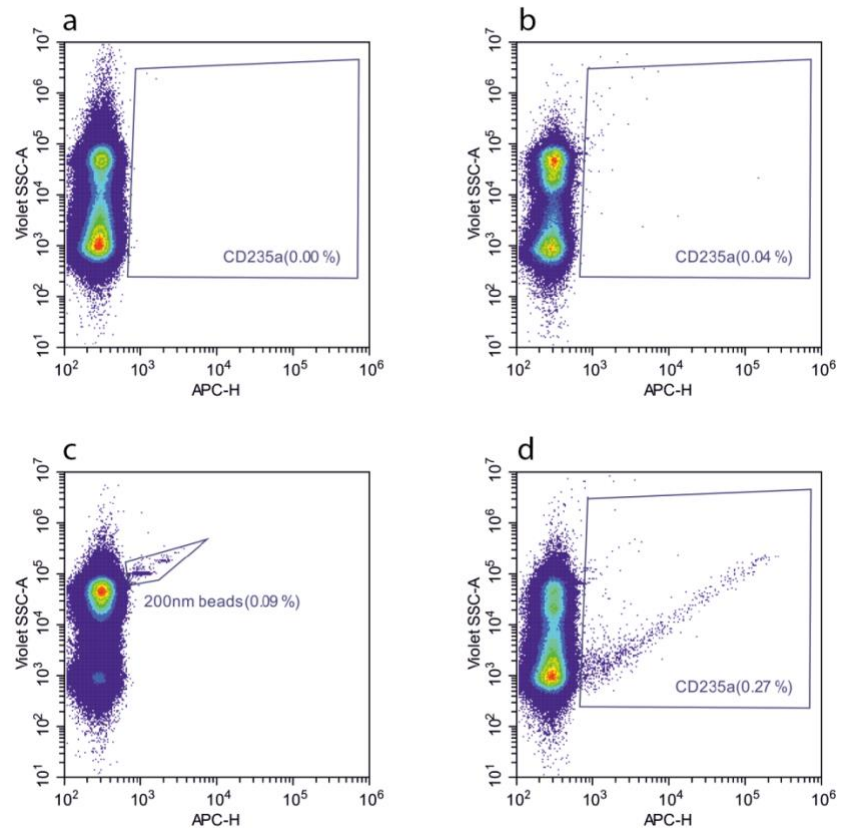
● Patients

d**e**

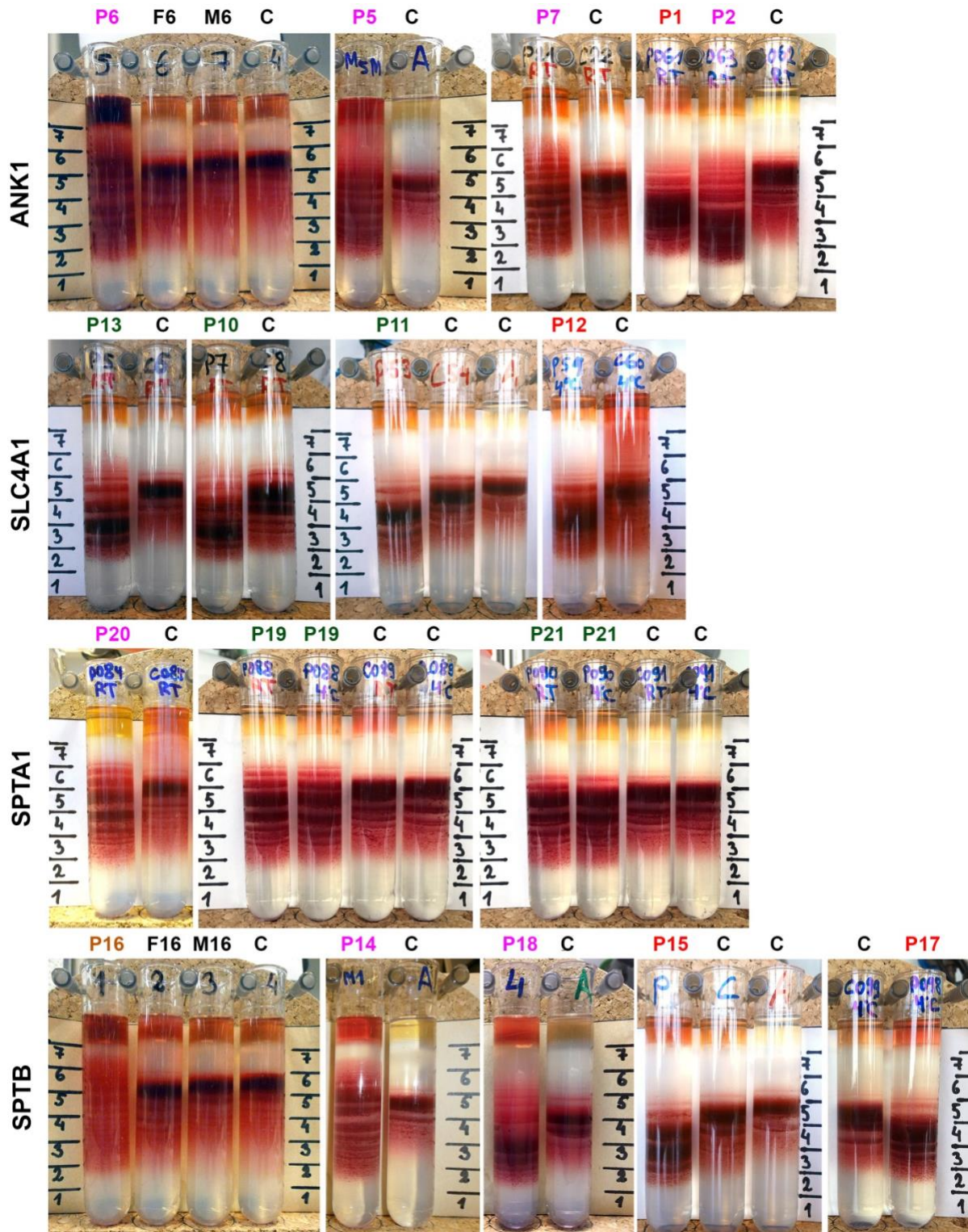




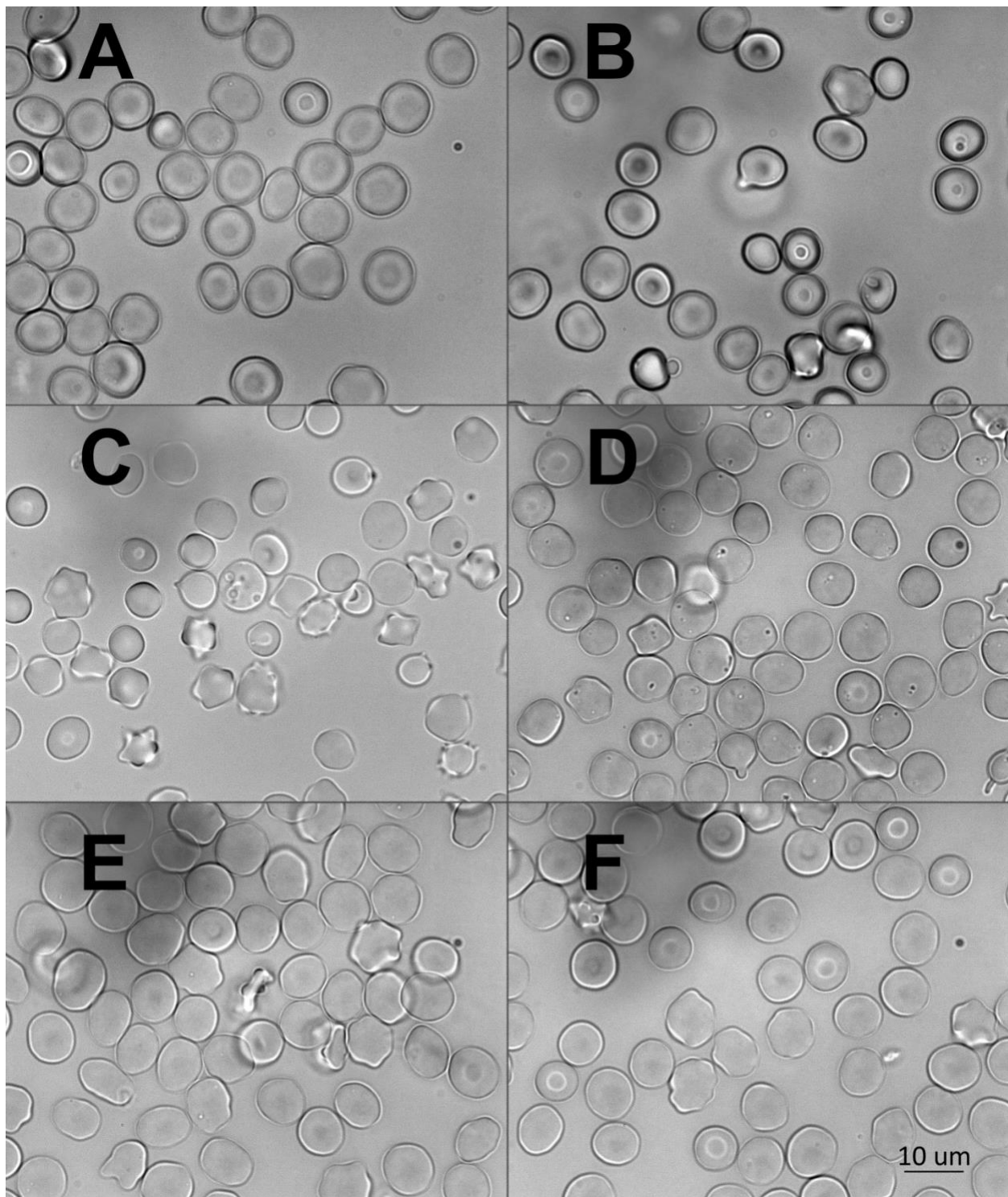
Supplemental Figures and Tables



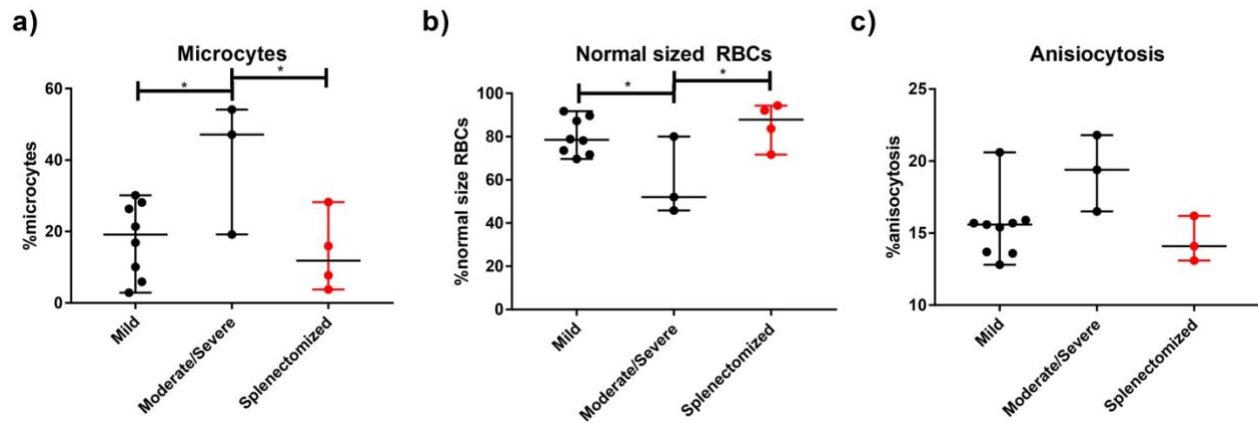
S.Fig 1: Panel a, b, c and d indicate gating strategies to detect RBC vesicles in plasma. A) Patient plasma diluted in PBS b) CD235a-APC diluted in PBS c) 200nm Ultra Rainbow Fluorescent Beads (Spherotech, Inc.) diluted in PBS d) representative APC-H vs. Violet plot of patient sample (plasma + CD235a-APC).



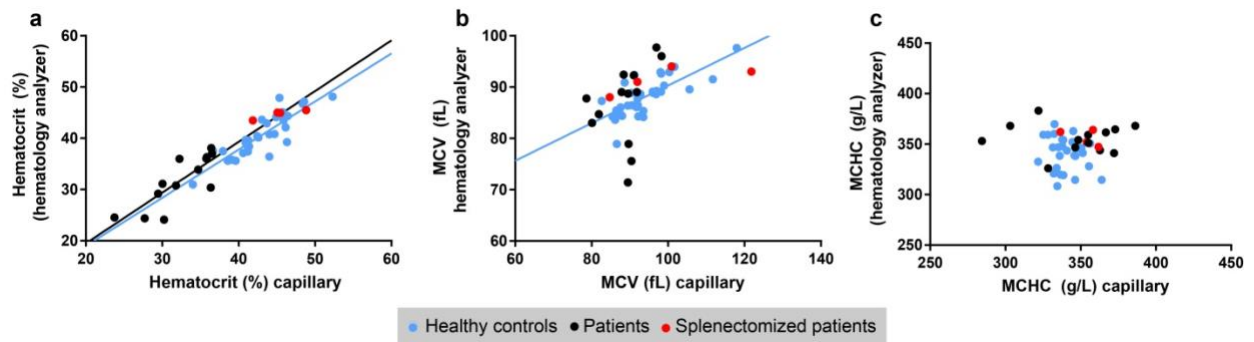
S.Fig 2: HS RBCs separated on the 90 % Percoll density gradient compared to co-transported controls. Mild clinical severity is marked in dark-green, moderate – in pink, severe - in orange, splenectomized – in red, controls and unaffected relatives marked in black. F - father of the patient, M – mother of the patient. Control blood sample to P12 was partially frozen during the transportation.



S.Fig 3: Representative life images of RBC resuspended in plasma-like buffer. A – cells from P19, mild anemia, B – cells from P7, moderate anemia, C – cells from P2, severe anemia, D – cells from splenectomized P1, E and F – cells from two co-transported controls.



S.Fig 4: %microcytes, %normal sized RBCs and %anisocytosis in mild, moderate/severe and splenectomized HS measured by digital microscopy.



S.Fig 5: correlations between automated and capillary measurements of hematocrit, MCV and MCHC. In blue dots healthy controls, black dots HS patients and red dots splenectomized HS patients dots patient are depicted. Statistical significant correlations are displayed with linear regression lines. a) correlations between automated hematocrit and capillary hematocrit measurements b) correlations between automated MCV and capillary MCV measurements, d) correlations between automated MCHC and capillary MCHC measurements

Supplemental methods

Subjects

Patients diagnosed with HS were enrolled in the CoMMiTMenT-study (<http://www.rare-anaemia.eu/>) after spoken and written informed consent. This study was approved by the Medical Ethical Research Board of the University Medical Center Utrecht, the Netherlands, (UMCU) under reference code 15/426M 'Disturbed ion homeostasis in hereditary haemolytic anaemia' and by the Ethical Committee of Clinical Investigations of Hospital Clinic, Spain, (IDIBAPS) under the reference code 2013/8436. HS patients were included in the study after confirming the diagnosis of HS with gold standard techniques (i.e. osmotic gradient ektacytometry, osmotic fragility test, EMA-binding, microscopy¹) and DNA analysis by Next Generation Sequencing. In brief, seven genes commonly associated with RBC membrane disorders were analyzed: *SPTA1* (a-spectrin), *SPTB* (b-spectrin), *ANK1* (ankyrin), *SLC4A1* (Band 3), *EPB41* (protein 4.1), *EPB42* (protein 4.2), and *RHAG* (Rhesus-associated glycoprotein). After enrichment of genomic DNA, using a custom Agilent SureSelectXT probe kit, protein coding and flanking intronic sequences were determined using a SOLiD™-5500XL system. Variants were identified using an 'in house' developed NGS mapping and calling pipeline, and the Cartagenia BENCHlab NGS module was used for filtering and prioritization of possible pathogenic variants. Detected mutations were confirmed by conventional Sanger sequencing. Novel variants with a clear pathogenic nature (i.e. frameshift mutants, nonsense mutants, splice site mutations) were considered to be causal. All novel missense variants were tested for pathogenicity using commonly known prediction tools SIFT, PolyPhen-2, and MutationTaster. In addition, their occurrence in the healthy control population was investigated using Gnomad (<http://gnomad.broadinstitute.org>). Exclusion criteria were the use of erythrocyte transfusion in the last 90 days, age lower than three years and body weight lower than 18kg. After inclusion, HS patients were categorized to their genetic defect (i.e. *ANK1*, *SLC4A1*, *SPTA1* and *SPTB*) and to their clinical severity. Clinical severity in non-splenectomized HS patients was previously defined by Bolton-Maggs² on basis of

1) hemoglobin and 2) reticulocytes levels. Mild HS was defined as hemoglobin levels between 110–150 g/L, moderate HS as hemoglobin levels between 80–120 g/L and severe HS as hemoglobin levels lower than 80 g/L. HS patients with hemoglobin levels between 110 and 120 were categorized as mild or moderate on basis of their reticulocytes levels (i.e. lower or higher than 6% reticulocytes). Blood from healthy controls was anonymously obtained using the approved medical ethical protocol of 07/125 Mini Donor Dienst. Patient blood was shipped with blood from a healthy control overnight from the University Medical Center Utrecht (Utrecht, The Netherlands) and Institut d'Investigacions Biomèdiques August Pi i Sunyer/ Hospital Clínic de Barcelona (Barcelona, Spain) to Saar University (Homburg, Germany) and University of Zurich (Zurich, Swiss) in lithium-heparin tubes either at room temperature or at 4°C to perform advanced research tests³. Functional domains and protein lengths are obtained from Lux *et al.*, Satchwell *et al.*, Ding *et al.*, Barneaud-Rocca *et al.*, Yasunaga *et al.*, Bennett *et al.*^{4–9} and UniProt database (www.uniprot.org).

Hemocytometry analysis

Hemocytometry parameters (i.e. Hb, RBC numbers, hematocrit, MCV, MCH, MCHC, reticulocytes) were analyzed on the Abbott Sapphire cell analyzer (Abbott Diagnostics Division, Santa Clara, CA, USA) and ADVIA 2120 (Hematology System, Siemens Healthcare Diagnostics, Forchheim, Germany)

Capillary-based measurements of MCV and MCHC

Automated hematology measurements for hematocrit, MCV and MCHC can be affected various factors such as by shape, cell orientation and osmotic fragility¹⁰ and therefore were also measured by micro-capillaries. Also, we used capillary-based measurements of MCV and MCHC, because RBC density measurements by Percoll are known to correlate with RBC age¹¹. Hematocrit (hct) capillaries were filled with intact well-mixed heparinized blood samples. For each blood sample, hematocrit measurements were carried out in triplicate. Capillaries were centrifuged for 5 min at 12.000 rpm (Hematocrit 20,

Hettich Zentrifugen). The total height of the samples and packed RBC height in capillary was measured manually with 0.1 mm accuracy. Mean hematocrit was calculated for the triplicate measurements and an average hematocrit was taken. MCV was calculated using the formula; $MCV = \text{hematocrit} / [\text{RBC number}]$ and MCHC was calculated using the formula; $MCHC = [\text{Hemoglobin}] / \text{Hematocrit}$.

Intracellular potassium measurements

An aliquot lithium-heparin whole blood was directly stored at -80°C after blood collection. At the same time, an aliquot of lithium heparin plasma was obtained by centrifugation of whole blood at 1000g for 10 minutes. The obtained plasma was centrifuged again at 4000g for 10 minutes to remove debris and residual cells. At the day of analysis, the aliquot of whole blood underwent two additional freeze-thaw cycles in liquid nitrogen to ensure complete lysis. The hemolyzed whole blood and plasma samples were measured using the Instrumentation Laboratory IL943 Flame Photometer. Intracellular potassium ($[K^+]_{RBC}$) was calculated using the following formula;

$$[K^+]_{RBC} = \frac{[K^+]_{\text{whole blood}} - ([K^+]_{\text{plasma}} * (1 - \text{hematocrit}))}{\text{hematocrit}}$$

Pre-incubated osmotic fragility test and eosin-5-maleimide binding

For the osmotic fragility test, lithium heparinized whole blood was incubated for 24 hours at 37°C. Incubated whole blood was subsequently added to different concentrations of NaCl (pH=7.4) (Range 1.0 – 12.0 g/L). After 30 minutes of incubation, RBCs were spun down at 1250g for 5 minutes. The absorbance of the supernatants were measured at 540nm using a Spectramax ME2. Eosin-5-maleimide (EMA) binding was determined according to previously published protocols^{12–14}. Briefly, washed RBCs were incubated with 0.5 mg/ml eosin-5-maleimide and measured using the BD FACSCanto®. FITC signals

of EMA-bound RBCs from patients were percentual related to the average of EMA-signals from 6 healthy controls per measurement.

Osmotic gradient ektacytometry

Osmotic gradient ektacytometry measurements of RBCs from healthy controls and HS patients were obtained using the Omoscan module on the Lorrca MaxSis (Mechatronics, The Zwaag, The Netherlands). 250 μ L of whole blood was standardized to a hemoglobin concentration of 12.9 g/dL and injected in 5ml isotonic polyvinylpyrrolidone (PVP), and osmotic gradient ektacytometry was further carried out as previously described^{15–17}. Briefly, RBCs are subjected to constant shear stress (30 Pa.S) while the osmolarity gradually increases from \approx 80 mOsmol/L to \approx 550 mOsmol/L. During this increase in osmolarity, a refraction pattern is generated by a laser and this pattern is captured by camera. The accompanied software measures the elongation index (EI), which is calculated by $EI=(a-b)/(a+b)$. In this formula, a represents the length and b the width of the RBC population as observed in the refraction pattern. Representative osmotic gradient ektacytometry curves are depicted in grey in Fig 3a-d. In the osmotic gradient ektacytometry curve, three characteristic points are depicted. 1) EI_{max} represents the maximal deformability of the RBC population and is found whereas EI is maximal. 2) O_{hyper} (in mOsmol/L) represents the intracellular viscosity (or RBC density, or RBC hydration state) and is found at the hypertonic axis where the EI is 50% of EI_{max} . Lower values of O_{hyper} indicate increased intracellular viscosity and denser RBCs. 3) O_{min} (in mOsmol/L) correlates with the 50% lysis point in the manual OFT and is found at hypotonic conditions whereas EI_{min} is minimal. Higher values of O_{min} indicates increased osmotic fragility (or decreased osmotic resistance).

Separation on the Percoll density gradient

Intact blood samples (1 ml each) were layered over the 12 ml of 90% Percoll solution containing plasma-like components (mM) 140 NaCl, 4 KCl, 0.75 MgCl₂, 2 CaCl₂, 0.015 ZnCl₂, 0.2 alanine, 0.2 glutamate-Na, 0.2 glycine, 0.1 arginine, 0.6 glutamine, 10 glucose, 20 HEPES-imidazole, pH 7.40 RT, 0.1% BSA. Percoll density gradient and RBC separation were performed during the centrifugation at 50.000g for 15 min, no brakes (Sorvall RC 5C plus, rotor SM-24). To avoid RBC volume artefacts related to the cold-induced inhibition of Na/K pump, centrifugation was performed at 30-36°C temperature interval.

Tubes with the RBC separated within the Percoll density gradient were photographed in front of the homogeneous light source. Images were automatically analyzed by the Visio 4D software (Arivis AG) as follows: RBC density distribution profile within the tube was produced. From the density profile, several parameters describing each blood sample were determined. The density profile was divided in a fraction with young cells, medium cells (also defined as M fraction) and dense cells. Within the M fraction the number of RBC populations were counted and average RBC density was determined. The average RBC density was defined as the location of the most intense RBC fraction (a.u.) relative to total length of the Percoll gradient.

RBC production, heterogeneity and turn-over rate markers

CD71 was measured to investigate the effects of RBC turn-over and reticulocytosis on RBC density parameters, as CD71 is a marker of (early) reticulocytes and erythroblasts. CD71 on RBCs was measured using flow cytometry. Blood was resuspended in plasma-like media with pH=7.4 (in 10mM HEPES, 120mM NaCl, 5mM KCl, 2mM CaCl₂, 0.8mM MgCl₂). RBCs were incubated with mouse anti-human CD71-FITC (eBiosciences, clone OKT9). FITC IgG1 isotype control antibody was used from eBiosciences.

Samples were measured using a BD FACS Canto II. HbA1c levels were measured in order to acquire information about RBC clearance¹⁸. HbA1c levels were measured using the Menarini/ARKRAY HA-8180V

RBC vesicles measurements

RBC vesicles in plasma were measured using a new generation flow cytometer, because RBC vesiculation is considered to increase RBC density and to cause the reduced surface-area-to-volume in HS^{19–21}. Blood for RBC vesicle analysis was collected in CDPA (citrate phosphate dextrose adenine) additive solution³. Plasma was pipetted to new clean tubes after centrifugation for 10 minutes at 1000g. Cell debris and residual cells were removed from plasma after an additional centrifugation step (10 min, 4000g) and plasma was subsequently aliquoted and stored at -80°C awaiting for further analysis. RBC vesicles were measured using the Beckman Coulter CytoFLEX flow cytometer. RBC vesicles were stained with 50µg/ml mouse anti-human CD235a-APC (BD Biosciences) with an equal volume of 25 times diluted CDPA plasma in 0.2µM filtered PBS. After incubation in the dark for 30 minutes, samples were additionally 40 times diluted in 0.2µM filtered PBS and measured by flow cytometry for 6 minutes with a flow speed of 10µL/min. RBC vesicles were measured using SSC-violet-H vs. APC-H (allophycocyanin-H), and thresholds were set using blanks, plasma dilution samples with anti IgG2bk-APC and 200nm Ultra Rainbow Fluorescent Beads (Spherotech, Inc.), see S.Fig 1. Events positive for APC-H were considered to be RBC-vesicles. RBC-vesicle concentrations were standardized to RBC numbers in blood (particles/10¹² RBC/L plasma).

RBC morphology evaluation with light microscopy and digital microscopy

1,5 – 2 µl of intact blood was resuspended in 1 ml of plasma-like buffer containing 0.1% of bovine serum albumin. Then cell suspension was pipetted inside the microscopy chamber with the glass bottom. Cells were allowed to precipitate for 5-7 min and then microscopy images were taken by Zeiss Axiovert

inverted microscope using 100x objective.

Statistical analysis and correlations

Statistical analysis was carried out using Graphpad Prism 7.02 and IBM SPSS Statistics 21. One-Way ANOVA with Post-Hoc correction (Tukey) was used to test for significant differences between healthy controls and HS patients. Also, HS patients with different genotypes were tested to each other and to healthy controls. Significant levels of $P \leq 0.05$ were considered to reflect significant differences. In figures and figure legends significant differences are more specifically noted with * ($P \leq 0.05$), † ($P \leq 0.01$) or ‡ ($P \leq 0.001$). Reference values are depicted in gray and were obtained from laboratory references values or calculated using $\text{mean} \pm (1.96 * \text{SD})$ in healthy controls. Correlations were fitted with linear regression and correlations were considered significant when $P \leq 0.05$. Genotype-phenotype correlations were only carried out for unsplenectomized HS patients (Fig 3). In addition, in all figures splenectomized patients are depicted with red dots and were analyzed separately. Fisher's Exact Test was carried whether the phenotypes mild and moderate/severe were equally distributed along the different genotypes (*ANK1*, *SLC4A1*, *SPTB*, *SPTA1*). For Fisher's Exact Test we categorized the splenectomized patients as moderate/severe.

Reference list supplemental figures and methods

1. Bianchi P, Fermo E, Vercellati C, et al. Diagnostic power of laboratory tests for hereditary spherocytosis: a comparison study in 150 patients grouped according to molecular and clinical characteristics. *Haematologica* 2012;97(4):516–23.
2. Bolton-Maggs PHB, Langer JC, Iolascon A, Tittensor P, King M-J, General Haematology Task Force of the British Committee for Standards in Haematology. Guidelines for the diagnosis and management of hereditary spherocytosis - 2011 update. *Br J Haematol* 2012;156(1):37–49.
3. Makhro A, Huisjes R, Verhagen LP, et al. Red Cell Properties after Different Modes of Blood Transportation. *Front Physiol*;7.
4. Lux SE. Anatomy of the red cell membrane skeleton: unanswered questions. *Blood* 2016;127(2):187–99.
5. Satchwell TJ, Hawley BR, Bell AJ, Ribeiro ML, Toye AM. The cytoskeletal binding domain of band 3 is required for multiprotein complex formation and retention during erythropoiesis. *Haematologica* 2015;100(1):133–42.
6. Ding Y, Casey JR, Kopito RR. The major kidney AE1 isoform does not bind ankyrin (Ank1) in vitro. An essential role for the 79 NH2-terminal amino acid residues of band 3. *J Biol Chem* 1994;269(51):32201–8.
7. Barneaud-Rocca D, Etchebest C, Guizouarn H. Structural model of the anion exchanger 1 (SLC4A1) and identification of transmembrane segments forming the transport site. *J Biol Chem* 2013;288(37):26372–84.
8. Yasunaga M, Ipsaro JJ, Mondragón A. Structurally similar but functionally diverse ZU5 domains in human erythrocyte ankyrin. *J Mol Biol* 2012;417(4):336–50.
9. Bennett V. Ankyrins. Adaptors between diverse plasma membrane proteins and the cytoplasm. *J Biol Chem* 1992;267(13):8703–6.
10. Bull B, Koepke J, Simson E, van Assendelft O. Procedure for Determining Packed Cell Volume by the Microhematocrit Method; Approved Standard—Third Edition.
11. Bosch FH, Werre JM, Roerdinkholder-Stoelwinder B, Huls TH, Willekens FL, Halie MR. Characteristics of red blood cell populations fractionated with a combination of counterflow centrifugation and Percoll separation. *Blood* 1992;79(1):254–60.
12. King MJ, Behrens J, Rogers C, Flynn C, Greenwood D, Chambers K. Rapid flow cytometric test for the diagnosis of membrane cytoskeleton-associated haemolytic anaemia. *Br J Haematol* 2000;111(3):924–33.
13. King M-J, Telfer P, MacKinnon H, et al. Using the eosin-5-maleimide binding test in the differential diagnosis of hereditary spherocytosis and hereditary pyropoikilocytosis. *Cytometry B Clin Cytom* 2008;74(4):244–50.
14. Huisjes R, Satchwell TJ, Verhagen LP, et al. Quantitative measurement of red cell surface protein expression reveals new biomarkers for hereditary spherocytosis. *Int J Lab Hematol* 2018;40(4):e74–e77.

15. Da Costa L, Suner L, Galimand J, et al. Diagnostic tool for red blood cell membrane disorders: Assessment of a new generation ektacytometer. *Blood Cells, Mol Dis* 2016;56(1):9–22.
16. Lazarova E, Gulbis B, Oirschot B van, van Wijk R. Next-generation osmotic gradient ektacytometry for the diagnosis of hereditary spherocytosis: interlaboratory method validation and experience. *Clin Chem Lab Med* 2017;55(3):394–402.
17. Huisjes R, Bogdanova A, van Solinge WW, Schiffelers RM, Kaestner L, van Wijk R. Squeezing for Life – Properties of Red Blood Cell Deformability. *Front Physiol* 2018;9:656.
18. Lutz HU, Bogdanova A. Mechanisms tagging senescent red blood cells for clearance in healthy humans. *Front Physiol* 2013;4:387.
19. Perrotta S, Gallagher PG, Mohandas N. Hereditary spherocytosis. *Lancet* 2008;372(9647):1411–1426.
20. Bosch FH, Werre JM, Schipper L, et al. Determinants of red blood cell deformability in relation to cell age. *Eur J Haematol* 1994;52(1):35–41.
21. Willekens FLA, Werre JM, Groenen-Döpp YAM, Roerdinkholder-Stoelwinder B, de Pauw B, Bosman GJCGM. Erythrocyte vesiculation: a self-protective mechanism? *Br J Haematol* 2008;141(4):549–556.